Suitability of Bundle Approximation in AC Loss Analysis of NbTi Wires: Simulations and Experiment

M. Lyly, E. Krooshoop, R. Lübkemann, S. Wessel, A. Stenvall, M. Dhalle, and R. Mikkonen

***Abstract*—Multifilamentary NbTi wires for ac applications are manufactured by embedding filament bundles into a metal matrix. In this stage of the manufacturing process, it is possible to affect the layout of the cross section and to choose whether to use few large or many small bundles in order to achieve a certain amount of filaments. All in all, up to 100 000 filaments are attainable for wire having the diameter of 1 mm. In this paper, ac loss measurements in external magnetic field on differently stacked NbTi samples are described. The measurements were performed in a LHe-cooled cryostat. The amplitude of the external field was varied between 250 mT and 3 T at frequencies of 0.02 and 0.12 Hz. We discuss possibilities to simulate the losses with finite element method. In particular, we concentrate on the filament bundle approximation and the possibilities to exploit it in the research and development process of new NbTi wires. In this approach, the filament bundles are considered as a homogenous mixture of matrix and superconducting filaments. According to the results, the bundle approximation greatly overestimates the losses. Furthermore, it should not be used for comparing, e.g., two wire structures where one has bundles of different size than the other. However, when considering how to situate the bundles on the cross section to achieve minimal ac loss, the bundle approximation can be a useful tool.**

***Index Terms*—AC loss, finite-element method (FEM), measurements, multifilamentary, NbTi, numerical modeling.**

I. Introduction

NBTI wires have been commercially available over 50 years. The manufacturing process of the wires is highly optimized and complex wire structures can be produced. In AC loss applications, twisted multifilamentary conductors having filament diameter below 10 μm are needed in order to achieve low enough losses [1]. Low AC losses result in reduced operation costs and increased stability margin. For example, in FAIR project, where the superconducting magnets are supposed to be ramped with several Teslas per second, the development of new low loss wires plays a crucial role [2].

The R&D process of a new wire is typically guided by analytical expressions for AC losses and the knowledge from the previous wires. However, even though the wires have been available for a long time, the manufacturing process and the proximity effect limit the adjustment of parameters, that would reduce the losses [1], [3]. One option, which is however not well known, is the effect of alteration of wire's cross-section layout on losses. The alteration of the layout affects the field distribution in the wire and therefore the losses.

The effect of layout alteration on the field distribution can be taken into account with numerical simulation methods. These methods are often based on the eddy current model (ECM) [4], the formulations of which can be solved using, e.g., integral methods or finite element method (FEM). Especially, H-formulated ECM with non-linear power-law resistivity has been successfully exploited for modeling AC losses in high temperature superconductors [5]–[7]. When trying to simulate twisted multifilamentary wires with FEM, the discretization of the complex structure on the filament level, however, easily results in a non-practical simulation time.

In this paper, we present the AC loss measurement results for three different NbTi wires. Additionally, we discuss the possibilities to exploit FEM in the AC loss simulations of these complex wires. Particularly, we consider the usability of the filament bundle approximation and the time-harmonic approach in the R&D process of the NbTi wires. In the filament bundle approximation, the filament bundles are considered as a homogenous domain instead of individual filaments and matrix [8], [9]. The time-harmonic approach is used to approximate the losses in the matrix due to the interbundle coupling currents [10]. In this approach, the bundles are presented with linear material properties.

II. Measurement Setup

The losses in the NbTi samples due to the external magnetic field were measured with a pick-up coil system, located in the University of Twente, Enschede, Netherlands [11]. The schematic view of the system is shown in Fig. 1. In this setup, the cylindrically wound sample is placed in the sample space and external field is applied with the superconducting AC magnet. A typical sample coil consists of 14–17 turns within diameter of 38–44 mm. The superconducting pick-up coils register the changes in the time-varying field as induced voltage. The voltage consists of the induced voltage due to the applied field and the part covering the losses in the sample and in the environment. The purpose of the inner pick-up coil is to improve the accuracy of the system.

In order to suppress the effect of the applied field, the pick-up system consists of the upper part and the identical lower part which are connected in series with the opposite winding directions. Further, to reduce the influence of the environment, the losses are measured without the sample and subtracted from the losses with the sample.

Manuscript received August 11, 2014; accepted November 18, 2014. Date of publication December 4, 2014; date of current version February 6, 2015.

M. Lyly, A. Stenvall, and R. Mikkonen are with the Tampere University of Technology, 33101 Tampere, Finland (email: mika.lyly@tut.fi).

E. Krooshoop, R. Lübkemann, S. Wessel, and M. Dhalle are with the University of Twente, 7500 Enschede, The Netherlands.

Color versions of one or more of the figures in this paper are available online at http://ieeexplore.ieee.org.

Digital Object Identifier 10.1109/TASC.2014.2376184

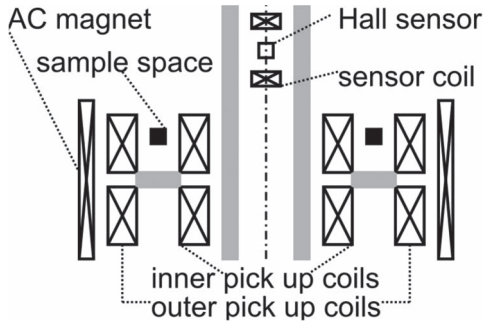

Fig. 1. Schematic view of the coils and sample space in AC loss measurement system [11].

In this setup, the superconducting sensor coil with the Hall sensor, located in the field free region, is used to deliver the signal of the pick-up circuit to the computer. The setup and the sample were cooled with liquid helium.

III. Computational Model

Both the hysteresis loss in the superconducting filaments and the losses in the metal matrix can be interpreted as ohmic losses [12]. In this paper, the computation is based on the eddy current model (ECM) [4]. We utilized in the H-formulation in 2-D for the hysteresis losses and the $A-v$-formulation in 3-D for the eddy current and coupling losses.

In the 2-D simulations, the resistivity in the superconducting regions, $\rho_{\rm sc}$, was applied via power law

$$\rho_{\rm sc} = \frac{E_{\rm c}}{J_{\rm c}} \left(\frac{|J|}{J_{\rm c}} \right)^{n-1} \tag{1}$$

where $E_{\rm c}$, $J_{\rm c}$, $|J|$, and n are the critical electric field criterion (0.1 μV/cm), the critical current density, the modulus of the current density, and the superconductor index value (50), respectively. Air was modeled as a high resistivity region having a resistivity of 0.1 Ωm. This has negligible effect on the losses in conductors [13]. In the whole modeling domain, the permeability was equal to the permeability of free space, μ_0. The bundles were modeled as a homogenous mixture of superconducting filaments and the matrix and the resisitivity in the individual bundle was set as

$$\rho_{\rm b} = \frac{1}{\lambda_{\rm sc}\rho_{\rm sc}^{-1} + (1-\lambda_{\rm sc})\rho_{\rm m}^{-1}} \tag{2}$$

where $\lambda_{\rm sc}$ and $\rho_{\rm m}$ are the fraction of superconductor and the resistivity of the matrix in the bundle, respectively.

In the 3-D simulations, the losses in the matrix were approximated with the time-harmonic approach introduced in [10]. In this approach, the superconducting bundles are modeled as a material having a linear resistivity

$$\rho_{\rm lin} = \delta^2 \pi f \mu_0 \tag{3}$$

where $\delta = k r_{\rm b}$ is the scaled penetration depth, and $r_{\rm b}$ is the radius of a bundle. The parameter $k = 2.25$ was chosen according to the benchmark simulations of the time-harmonic approach presented in [10].

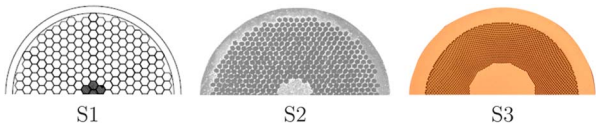

Fig. 2. One half of the NbTi wire cross sections. In S1, the dark region represents filament free region. In S1 and S2, each visible filament bundle consist of 85 and 55 filaments, respectively. In S3, the dark zone consists of 3858 filaments.

The dissipated energy [J] per cycle was computed by integrating the power as

$$W = \iint_{T\,\Omega} E \cdot J \, d\Omega \, dt \tag{4}$$

where T and Ω are the period and the domain, respectively.

The measurements were also compared to analytical solutions. According to [14], the solution for hysteresis loss [J] per cycle in a round superconducting filament under time-varying external magnetic field perpendicular to the wire's axis is

$$Q_{\rm h} = 2\frac{8}{3\pi} r_{\rm f} J_0 B_0 \ln\left(\frac{\hat{B}+B_0}{B_0} \right) V_{\rm sc} \tag{5}$$

where $r_{\rm f}$, $\hat{B}$, and $V_{\rm sc}$ are the radius of filament, the amplitude of the magnetic flux density, and the volume of superconductor, respectively. The equation is valid for a wave varying between $-\hat{B}$ and $\hat{B}$. The parameters J_0 and B_0 define the critical current of the wire as [14]

$$J_{\rm c} = \frac{J_0 B_0}{B + B_0}. \tag{6}$$

The losses in the matrix [J] per cycle can be solved as [15]

$$Q_{\rm m} = \frac{B_{\rm m}^2}{2\mu_0} \frac{8\tau}{T_{\rm m}} V_{\rm w} \tag{7}$$

where $\tau = \mu_0/(2\rho_{\rm et})(L/(2\pi))^2$ is the time constant. The symbols $B_{\rm m}$, $V_{\rm w}$, $\rho_{\rm et}$, and L are the peak-to-peak value of the magnetic flux density, the volume of the wire, the effective transverse resistivity of the matrix, and the twist pitch of the wire, respectively. $T_{\rm m}$ is the rise time from $-\hat{B}$ to $\hat{B}$. The equation is valid for a triangular wave. Since it is not straightforward to calculate $\rho_{\rm et}$, we used the average values measured for a multifilamentary NbTi wire for RHIC accelerator in [3]. Various other analytical solutions, taking into account e.g., the center copper, have been presented in [15].

IV. Wire Samples and Measurements

Fig. 2 and Table I show the cross-section layouts of the investigated wires and their geometrical data, respectively. In Table I, the symbols $N_{\rm b}$, $N_{\rm f}$, $d_{\rm w}$, α, $A_{\rm sc}$ are the number of bundles, the number of filaments, the diameter of wire, the ratio of matrix to superconductor in the wire, and the area of superconductor in wire cross-section. In single stacking process, monofilaments are embedded in the matrix [16].

All the wires were measured at applied external magnetic field, varying triangularly in time around zero offset. Measurements were done for $\hat{B}$ of 0.25, 0.375, 0.5, and 3 T,

TABLE I
DATA OF THE WIRE CONFIGURATIONS. S STANDS FOR SINGLE STACK

sample	N_b	N_f	r_f [μm]	d_w [mm]	α	L [mm]	A_sc [mm^2]
S1	294	24990	1.70	0.798	1.360	7.20	0.212
S2	714	39270	1.35	0.819	1.624	6.60	0.201
S3	s	3858	3.55	0.763	2.075	15.5	0.149

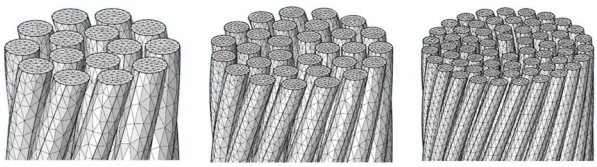

(a) (b) (c)

Fig. 3. Various modeling domains of S2. Only the filament bundles are shown. The amounts of bundles are (a) 15, (b) 30, and (c) 60, respectively.

TABLE II
GEOMETRICAL PARAMETERS OF SAMPLE S1 AND SAMPLE S2 FOR DIFFERENT N

sample	N	N_b	α_b	N_l	r_b [mm]
S1	12	25	0.7	3	0.060
	5	59	0.7	4	0.039
S2	48	15	0.7	2	0.076
	24	30	0.7	3	0.054
	12	60	0.7	4	0.038

with the ramp rates of 120, 180, and 240 mT/s (system maximum) for the two latest, respectively. This resulted in frequencies of 0.12 and 0.02 Hz, for the first three and the fourth amplitude, respectively.

V. SIMULATIONS

Since the wires have thousands of filaments stacked as several hundreds of bundles, their detailed mesh representations, which could show the current penetration effect, would need such a high number of elements that FEM modeling becomes unpractical. Consequently, in the simulations we present the wires with the original number of bundles divided by factor N. Additionally, we consider the losses only in wires S1 and S2 to demonstrate the bundle approximation. S3 was measured to attain more perspective for the general behavior of losses.

The modeling domains with different values of N for S2 are presented in Fig. 3. The ones for S1 were similar. In Fig. 3, bundles are located in N_1 co-centric layers. The details of the geometries S1 and S2 are shown in Table II. In Table II, the symbols r_b and α_b are the radius of bundle and the ratio of matrix to superconductor in the bundle, respectively. Since the fractions N_b/N did not result to an integer, r_b was varied to maintain the correct α. The same α_b was used for all wires because the filaments were assumed to be stacked similarly despite the size of the bundle.

In the 2-D simulations, the cross-section layouts of bundles were the same as in Fig. 3. However, r_b was altered in order to keep α the same. The same element size meshing parameter was used in the individual bundles when N was varied.

In the simulations, J_c was approximated with (6). For S1 and S2 B_0 was 1.559 and 1.539 T, respectively. J_0 was 12 GA/m^2

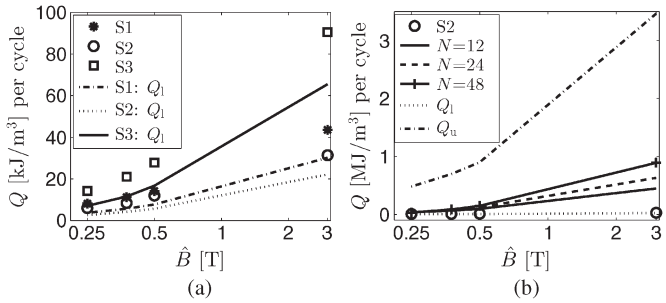

Fig. 4. Measured AC losses in the samples and the analytical solutions.

for both wires. The parameters were based on the critical current measurements of the wires. The average values for ρ_m at 0.25, 0.375, 0.5, and 3 T amplitudes were 0.443, 0.444, 0.445, and 0.667 nΩm, respectively [3]. All 2-D simulations were done at the frequency of 50 Hz. At 50 Hz the numerical simulations based on H-formulated ECM agree well with the analytical formulae and experiments [13], [5]. Additionally, 2-D geometries are only used for computing hysteresis losses, which are frequency independent per cycle.

Additionally, the simulations were compared to the analytical solution at the lower and upper limit (Q_l and Q_u). Q_l was calculated by adding to the losses in the matrix [see (7)], the hysteresis losses of N_f non-interacting filaments having the radius of r_f according to (5). In the computation of Q_u, hysteresis losses were calculated by assuming one large filament with the cross-sectional area of A_sc shown in Table I. Losses in the matrix were included in Q_u similarly like in Q_l.

VI. RESULTS AND DISCUSSION

Fig. 4(a) shows the measured AC losses of the wires as a function of $\hat{B}$. The losses in S1 and S2 were closer to each other, because the amount of superconductor and the filament size were at the same range. The losses were the smallest in S2 due to the smallest filaments and twist pitch (see Table I). In S3, the losses were the highest due to the largest r_f and L. Also, the analytical solution predicted that the losses were always the lowest in S2 and the highest in S3.

Fig. 4(b) shows the AC losses in S2 as a function of $\hat{B}$. Also, the simulated losses with the different values of N, Q_l, and Q_u are shown. According to the results, the bundle approximation resulted in losses closer to the upper limit than the experiments. When using the bundle approximation, all the filaments in the individual bundles are assumed to be coupled. Since the measured losses in the wires are close to the lower limit, when no coupling is assumed, it is clear that the bundle approximation overestimates the losses, but still gives more reasonable upper limit than the analytical approach.

Table III presents the difference between the measured losses and the numerical results for S1 and S2. The bundle approximation predicted 5–20 times higher losses than was measured. Even though the approximation with $N = 5$ for S1 was already relatively close to the geometry where each bundle could be presented, the losses were 5–12 times higher than the measured losses. This indicates that the bundle approximation would

TABLE III
LOSSES WITH BUNDLE APPROXIMATION DIVIDED BY THE MEASURED LOSSES

$\hat{B}$ [T]	0.25	0.375	0.5	3
S1, N=12	4.9052	8.2558	10.2483	17.7402
S1, N=5	4.8621	6.5597	7.6640	11.5879
S2, N=24	6.1022	9.4573	10.2563	20.0952
S2, N=12	5.9474	7.7990	7.9731	14.2598

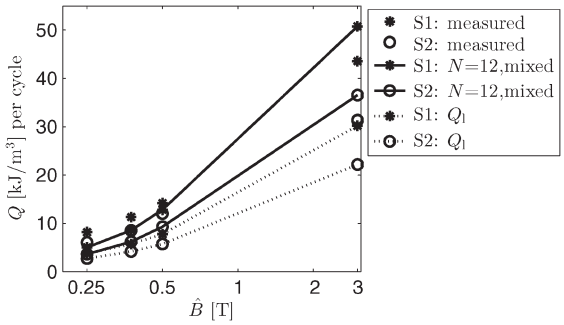

Fig. 5. Measured losses in S1 and S2 with mixed solutions.

TABLE IV
LOSSES WITH MIXED SOLUTION DIVIDED BY THE MEASURED LOSSES

$\hat{B}$ [T]	0.25	0.375	0.5	3
S1	0.6129	0.7587	0.9045	1.1654
S2	0.5984	0.7273	0.7744	1.1644

greatly overestimate the results even though all the bundles could be modeled as homogenous material.

Fig. 5 presents the measured losses in S1 and S2 with mixed solutions as a function of $\hat{B}$. For the mixed solutions, the hysteresis losses were computed with (5) by assuming non-interacting filaments and the losses in the matrix with the time-harmonic approach. The differences between the measurements and simulations are shown in Table IV. When compared to the measurements, the losses of mixed solutions were 40% lower and 17% higher for the field amplitudes of 0.25 and 3 T, respectively. The difference with measurements and the faster increase in simulated losses as a function $\hat{B}$ can partially be caused by erroneous estimate for the field dependent ρ_{m} and partially due to the harmonic excitation in 3-D simulations.[1]

Even though the difference between the simulations and measurements changed when $\hat{B}$ was varied, the change was similar for both samples. Also, the simulations predicted that the losses were always higher in S1 than in S2, which agrees with the measurements. Therefore, the mixed approach can be useful in R&D process of new wires, when various wire structures are compared.

Finally, the simulated losses in the matrix for S2 are shown in Table V. In simulation cases 1–3, the distances between the bundle layers and the radii of the bundle free core were approximately the same. In case 4, the bundles were located closer to the center of the wire. Fig. 6 shows the cross-section layouts

[1]Instead of time-harmonic modeling, also a linear transient problem with a triangular excitation could be solved. However, this would result in significantly higher simulation times and was not included in this study.

TABLE V
SIMULATED LOSSES IN THE MATRIX [kJ/m^3] PER CYCLE FOR S2

case	$\hat{B}$ [T]	0.25	0.375	0.5	3
1	$N = 48$	1.102	2.473	4.387	19.060
2	$N = 24$	1.083	2.430	4.311	17.332
3	$N = 12$, loose	1.197	2.687	4.766	19.091
4	$N = 12$, close	1.382	3.102	5.502	22.026

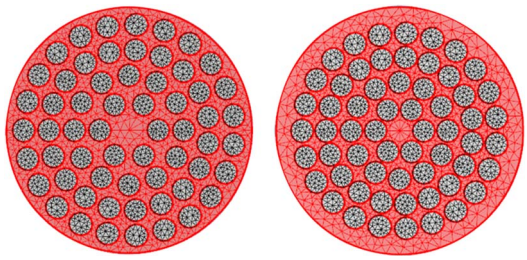

Fig. 6. (Left) Loose and (right) close packing of bundles.

in cases 3 and 4. According to the results, the subdivision of bundles had smaller influence on the losses than the variation in the location of bundles. This seems reasonable because when the filaments were closely packed, the path for interfilamentary currents was more narrow and current density increased. Similar behavior was noticed in [10]. The simulations indicate that by a correct layout design of bundles, lower AC losses could be attained. Therefore, when considering the R&D process, by presenting the wire at the bundle level, the best layout for certain number of bundles could be searched.

VII. CONCLUSION

In this paper, AC loss measurements of three twisted multifilamentary NbTi samples were decribed. The measurements were performed in external magnetic field. The losses were simulated by using filament bundle approximation and FEM.

According to the results, the filament bundle approximation greatly overestimates the hysteresis loss because it assumes fully coupled filaments inside the bundle. Consequently, it should not be used for comparing e.g. two wire structures where the one has bundles of different size than the other. Simulated losses were 5–20 times higher than the measured losses due to the too high hysteresis loss.

The losses were also considered with mixed solutions where the hysteresis losses of the filaments and the losses in the matrix were computed analytically and with the time-harmonic approach in 3-D, respectively. The losses were within 40%. However, the difference was similar for different wires.

In summary, the bundle approximation should not be used in comparison of wire structures having bundles of different sizes. However, when considering the search of the best layout for certain amount of bundles, the bundle approximation could be a useful tool. In the preliminary studies of R&D process of new wires, where the different wire structures are compared, mixed approach is proposed instead of bundle approximation. However, more studies are needed in order to find out how small geometrical differences this approach can register. In this paper, the geometrical differences of the wire samples were relatively clear.

REFERENCES

[1] M. Lyly, M. Holm, A. Stenvall, and R. Mikkonen, "Design process for a NbTi wire with new specification objectives: Technical design constraints and optimization of a wire layout considering critical current and ac losses," *IEEE Trans. Appl. Supecond.*, vol. 23, no. 1, Feb. 2013, Art. ID. 6000910.

[2] P. Spiller and G. Franchetti, "The FAIR accelerator project at GSI," *Nucl. Instrum. Methods Phys. Res. Section A, Accel., Spectrometers, Detectors Assoc. Equip.*, vol. 561, no. 2, pp. 305–309, Jun. 2006.

[3] M. Wilson, "NbTi superconductors with low ac loss: A review," *Cryogenics*, vol. 48, no. 7/8, pp. 381–395, Aug. 2008.

[4] O. Biro, "Edge element formulations of eddy current problems," *Comput. Methods. Appl. Mech. Eng.*, vol. 169, no. 3/4, pp. 391–405, Feb. 1999.

[5] Z. Hong, Q. Jiang, R. Pei, A. Campbell, and T. Coombs, "A numerical method to estimate ac loss in superconducting coated conductors by finite element modelling," *Supercond. Sci. Technol.*, vol. 20, no. 4, pp. 331–337, Apr. 2007.

[6] F. Grilli, R. Brambilla, F. Sirois, A. Stenvall, and S. Memiaghe, "Development of a three-dimensional finite-element model for high-temperature superconductors based on the H-formulation," *Cryogenics*, vol. 53, pp. 142–147, Jan. 2013.

[7] F. Grilli *et al.*, "Computation of losses in HTS under the action of varying magnetic fields and currents," *IEEE Trans. Appl. Supercond.*, vol. 24, 2014, Art. ID. 8200433.

[8] N. Amemiya, S. Murasawa, N. Banno, and K. Miyamoto, "Numerical modelings of superconducting wires for ac loss calculations," *Phys. C, Supercond.*, vol. 310, no. 1, pp. 16–29, 1998.

[9] M. Lyly, A. Stenvall, and R. Mikkonen, "Validation of homogenized filament bundle model in ac loss computations," *IEEE Trans. Appl. Supercond.*, vol. 22, no. 3, Jun. 2012, Art. ID. 4705505.

[10] M. Lyly, V. Lahtinen, A. Stenvall, L. Rostila, and R. Mikkonen, "A time-harmonic approach to numerically model losses in the metal matrix in twisted superconductors in external magnetic field," *IEEE Trans. Appl. Supercond.*, vol. 24, no. 2, Apr. 2014, Art. ID. 8200909.

[11] M. Woundstra, "Electromagnetic characterization of BSCCO-2212 multifilament wires," M.S thesis, Appl. Supercond. Centre, Faculty Appl. Phys., University of Twente, Enschede, The Netherlands, 1995.

[12] A. Bossavit, "Remarks about hysteresis in superconductivity modelling," *Phys. B, Condens. Matter*, vol. 275, pp. 142–149, 2000.

[13] V. Lahtinen, M. Lyly, A. Stenvall, and T. Tarhasaari, "Comparison of three eddy current formulations for superconductor hysteresis loss modelling," *Supercond. Sci. Technol.*, vol. 25, no. 11, Nov. 2012, Art. ID. 115001.

[14] M. Wilson, *Superconducting Magnets*. Cary, NC, USA: Oxford Univ. Press, 1987.

[15] J. L. Duchateau, B. Turck, and D. Ciazynski, *Handbook of Applied Superconductivity*, B. Seeber, Ed. London, U.K.: CRC Press, 1998, ch. B 4.3.

[16] K. Mess, Schmuser, and S. Wolff, *Superconducting Accelerator Magnets*. Singapore: World Scientific, 1996, ch. 3, pp. 36–37.